Angewandte Chemie
Eine Zeitschrift der Gesellschaft Deutscher Chemiker

Supporting Information

MiniAp-4: A Venom-Inspired Peptidomimetic for Brain Delivery

Benjamí Oller-Salvia, Macarena Sánchez-Navarro, Sonia Ciudad, Marc Guiu, Pol Arranz-Gibert, Cristina Garcia, Roger R. Gomis, Roméo Cecchelli, Jesús García, Ernest Giralt, and Meritxell Teixidó**

anie_201508445_sm_miscellaneous_information.pdf

Table of contents

Supplementary Materials and Methods

General peptide synthesis. Protected amino acids were purchased from Iris Biotech, ChemMatrix resin from PCAS BioMatrix Inc and HATU (1-[bis(dimethylamino)-methylene]-1H-1,2,3-triazolo[4,5-b]pyridinium 3-oxid hexafluorophosphate) from GL Biochem Shanghai Ltd. Solvents were supplied by SDS and trifluoroacetic acid by Scharlau. Other chemicals were acquired from Sigma-Aldrich and were of the highest purity commercially available.

Peptides were obtained by Fmoc/*t*Bu solid-phase synthesis in a 250-μmol scale on Rink Amide-ChemMatrix resin using L-amino acids. Fmoc (9-fluorenylmethoxycarbonyl) was deprotected with 20% piperidine in DMF (dimethylformamide). The resin was washed with DMF (5 x 30 s) and DCM (dichloromethane) (5 x 30 s) between synthetic steps. For peptide elongation the protected amino acid (4 eq.) was activated using DIC (diisopropylcarbodimide) (4 eq.) and Oxima Pure (4 eq.) in DMF/DCM 1:1. The extent of coupling was assessed by the Kaiser colorimetric assay[1] for primary amines and using the chloranil test[2] for secondary amines. When recoupling was required, the protected amino acid (4 eq.) was activated with HATU (4 eq) and DIEA (*N,N*-diisopropylethylamine) (4 eq). Peptides were cleaved with concomitant removal of the side-chain protecting groups, using TFA (trifluoroacetic acid), H_2O, EDT (1,2-ethanedithiol) and TIS (triisopropylsilane) (95:2:2:1) if the sequence included cysteines or TFA, H_2O and TIS (95:2.5:2.5) if not. After cleavage of the peptides, the solvent was evaporated applying a stream of N_2. The residue was washed 3 times by suspension in tert-butyl methyl ether and subsequent centrifugation. The cleaved peptides were then dissolved in H_2O/MeCN (1:1) with 0.1% TFA and freeze-dried.

The oxidation of thiols to obtain disulfide bridges was performed under air. A 100 μM solution of each peptide was prepared in 10 mM bicarbonate buffer (pH 8.0) and the solution was stirred at 20 ºC during 24 h. After this time, the buffer was acidified with TFA to pH 2 and lyophilized. The reaction was monitored by HPLC, the Ellman´s test and MALDI-TOF MS.

Peptides were purified in a Waters system with MassLynx 4.1 software, a 2545 binary gradient module, a 2767 manager collector, a 2998 photodiode array detector and a

Sunfire C_{18} column (150 x 10 mm x 3.5 μm, 100 Å, Waters). The flow rate was 6.6 mL/min using MeCN (0.1% TFA) and H_2O (0.1% TFA). Purity was checked by analytical reverse-phase HPLC or UPLC. MALDI-TOF MS and LC-MS were used to confirm the identity of the compounds synthesized, and purity was assessed by HPLC-UV.

HPLC chromatograms were obtained on a Waters Alliance 2695 with an automatic injector and a photodiode array detector 2998 Waters (Waters, Milford, MA) using a Sunfire C_{18} column (100 x 4.6 mm x 5 μm, 100 Å, Waters) and software EmpowerPro 2. The flow rate was 1 mL/min using MeCN (0.036% TFA) and H_2O (0.045% TFA). 8-min linear gradients were used in all cases.

UPLC conditions: Acquity high class (PDA eλ detector, sample manager FNT and Quaternary solvent manager). Column Acquity BEH C_{18} (50 x 2 mm x 1.7 μm). The flow rate was 0.61 mL/min using MeCN (0.036% TFA) and H_2O (0.045% TFA). 2-min linear gradients were used in all cases.

The molecular weight of all the peptides synthesized were determined routinely using a MALDI-TOF/TOF Applied Biosystem 4700. 1 μL of peptide solution (0.1-1 mg/mL) mixed with 1 μL of α-cyano-4-hydroxycinnamic acid (ACH) matrix was seeded on the MALDI plate and air-dried. To prepare the matrix 10 mg of ACH were dissolved in 1 mL of MeCN/H_2O 1:1 (v/v) containing 0.1% TFA.

All peptides were also analyzed using a high-resolution mass spectrometer to obtain their exact mass. Samples were dissolved in 200 μL of H_2O:MeCN and diluted in H_2O:MeCN 1% formic acid for MS analysis. The analysis was performed in a LTQ-FT Ultra (Thermo Scientific) and the sample was introduced by automated nanoelectrospray. A NanoMate (Advion BioSciences, Ithaca, NY, USA) infused the samples through the ESI Chip, which consists of 400 nozzles in a 20 x 20 array. Spray voltage was 1.7 kV and delivery pressure was 0.3 psi. MS conditions were: NanoESI, positive ionization, capillary temperature 200 ºC, tube lens 119V, ion spray voltage 2 kV and m/z 100-2000 amu.

The content and ratio of amino acids present in each peptide sample were determined by ion exchange chromatographic analysis after acid hydrolysis. The hydrolysis was performed with 6 M HCl at 110ºC for 16 h. After that time, the sample was evaporated to dryness at reduced pressure. The residue was dissolved in 20 mM aqueous HCl, derivatized using the AccQ Tag protocol from Waters, and finally analyzed by ion exchange HPLC.

MiniAp-4 synthesis. MiniAp-4 was synthesized by Fmoc/*t*Bu solid-phase peptide synthesis incorporating Fmoc-L-Asp(OAll)-OH and Fmoc-L-Dap(Alloc)-OH (Iris Biotech). Before deprotecting *N*-terminal diaminopropyl Fmoc, Allyl and Alloc were removed using tetrakis(triphenylphosphine)palladium(0) (0.2 eq) and phenylsilane (20 eq) in DCM. 4 treatments of 20 min were performed and deprotection was assessed by cleavage of a small amount of resin and MALDI-TOF MS. Cyclization was achieved with DIC (4 eq) and Oxima Pure (4 eq) and monitored through the Kaiser test. Subsequently, the Fmoc group of diaminopropionyl residue was removed and either a reactive moiety was coupled (maleimide or cysteine) or the peptide was directly cleaved.

Conjugation to maleimide-cyanine5.5. MiniAp-4 was obtained by manual Fmoc/*t*Bu solid-phase peptide synthesis as described in the previous sections, and Fmoc-Cys(Trt)-OH was coupled at the *N*-termini in solid phase. After that, the peptide was cleaved and purified. Conjugation to cyanine5.5-maleimide (Lumiprobe) was performed in aqueous buffer. The cysteine- peptide (0.6 μmol, 60 μL water) was mixed with cyanine5.5-maleimide (9 μmol, 9 μL DMSO) and triethylamine (TEA, pH 7-8). The mixture was allowed to react for 30 min and purified by reverse-phase HPLC.

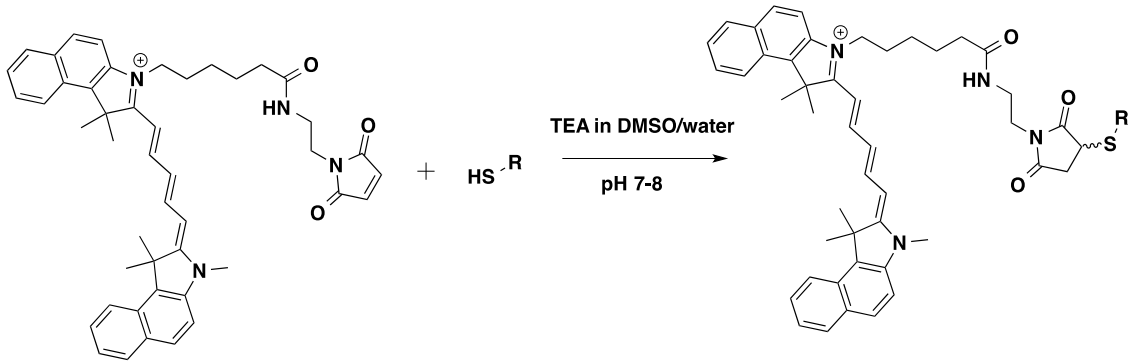

Scheme S1. Scheme of the conjugation of MiniAp-4 to GFP.

Circular dichroism . Circular dichroism spectra were recorded using a Jasco 810 UV-Vis spectropolarimeter, equipped with a CDF 426S/426L peltier. Samples were prepared as previously described for wild-type apamin.[3] Spectra were obtained between 190 and 250 nm, with a time response of 2 s, a scanning speed of 20 nm/min and a step resolution of 0.2 nm. Molar ellipticiy values were calculated from experimental ellipticity (in mdeg) using equation (3):

$$\theta = \frac{\theta_{exp}}{b \cdot C \cdot n} \qquad \textbf{(3)}$$

where θ is molar ellipticity in mdeg·cm^2·dmol^{-1}, θ_{exp} is measured ellipticity in mdeg, b is the optical path in cm, C is peptide concentration in M and n is the number of residues in the peptide.

NMR spectroscopy. NMR experiments were carried out on a Bruker Avance III 600 MHz spectrometer equipped with a TCI cryoprobe. Samples were prepared by dissolving peptides in 90% H_2O/10% D_2O at 3-4 mM and pH was adjusted to 2-3. Chemical shifts were referenced to internal sodium-3-(trimethylsilyl)propanesulfonate (DSS). The spectra of all analogs were acquired under the same conditions as a previous study of wild type apamin.[3] Suppression of the water signal was achieved by excitation sculpting.[4] Residue specific assignments were obtained from 2D total correlated spectroscopy (TOCSY) and correlation spectroscopy (COSY) experiments, while 2D nuclear Overhauser effect spectroscopy (NOESY) permitted sequence specific assignments. ^{13}C resonances were assigned from 2D ^{1}H-^{13}C HSQC spectra. All experiments were performed at 298 K except NOESY spectra that were acquired at 278 K. Amide proton temperature coefficients were determined from a series of one-dimensional spectra acquired between 278 and 308K. The TOCSY and NOESY mixing times were 70 and 250 ms, respectively.

Structures for MiniAp-1 were generated by the standard simulated annealing protocol implemented in the CNS software.[5] Only the distance restraints from inter-residue NOEs were used for the calculation. NOEs were classified as strong, medium and weak (upper limits for structure calculation were set as 2.5 Å, 3.5 Å and 4.5 Å, respectively). The necessary pseudoatom corrections were applied for non-stereospecifically assigned

protons at prochiral centers and for the methyl group of aliphatic side chains. The Φ and Ψ backbone torsion angle restraints included in the calculation were derived from experimental ^{1}H, ^{13}C and ^{15}N chemical shifts values using the PREDITOR server.[6] 80 structures were generated and 10 were selected based on lowest overall energy and on the basis of no violations of NOE or dihedral angle constraints greater than 0.2 Å and 5º, respectively. PROCHECK[7] was used to generate Ramachandram plot statistics of the final structures.

GFP modification. A solution of GFP (Millipore) (0.5 mg/mL) in sodium phosphate buffer (NaPi) (50 mM, pH 8, EDTA (ethylenediaminetetraacetic acid), 1 mM) was treated with 2-iminothiolane (10 eq, 2 mg/mL in H_2O) during 1 h at RT. The excess of reagent was removed by SEC (NAP-5, for volumes up to 0.5 mL, PDmiditrap for volumes up to 1 mL or PD10 for volumes up to 2.5 mL, GE Healthcare). The columns were previously equilibrated with reaction buffer following manufacturer instructions. Alkylation of the activated protein was performed by addition of 6 eq of selected maleimido peptide at RT for 1h. The resulting protein was purified by SEC and stored at 4ºC in PBS.

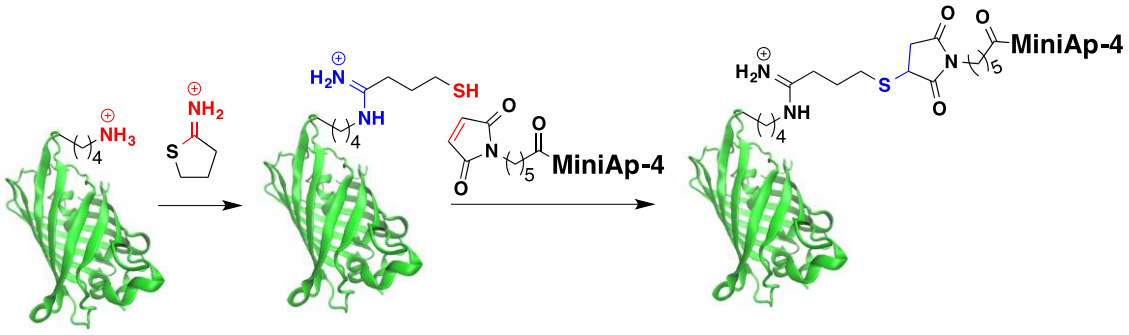

Scheme S2. Scheme of the conjugation of MiniAp-4 to GFP.

^{125}I protein labelling. Two Pierce™ Iodination Beads (Life technologies) were used for each protein. Briefly, beads were washed with reaction buffer (NaPi, 50 mM, pH 6.5) and dried on filter paper. In a glass vial, beads were added to a solution of carrier free Na^{125}I (approximately 1 mCi/mg protein) and incubated for 5 min. Proteins were added to the activated solution and the reaction was allowed to proceed for 15 min with occasional mixing. The reaction was stopped by removing the solution from the reaction vessel and adding it to a NAP-5 column (GE Healthcare) equilibrated with Ringer HEPES. Fractions of 250, 500, 250, 250 and 1000 μL were collected and radioactivity

of 10 μL fractions were measured for two min using Packard Cobra II Gamma Counter. BCA was used to determine the protein concentration.

Quantum dot modification. 1 μL of 0.4 M *N*-(γ-maleimidobutyryloxy)succinimide in DMF (400 nmol, 1000 eq) (Sigma-Aldrich) was diluted with 79 μL of 50 mM borate buffer pH 8. pH was readjusted to 8 with 0.1 M NaOH. This solution was mixed with 50 μL of 8 μM Amino PEG QDot 605 (0.4 nmol, 1 eq) (Life Technologies). The mixture was incubated for 1 h at room temperature under gentle shaking and was then separated with a NAP-5 column (GE Healthcare) eluting in PBS.

A 0.4 M solution of 80 μL of 0.4 M tris(2-carboxyethyl)phosphine (TCEP) was prepared in 100 mM phosphate buffer pH 8. 4 μL of this TCEP solution (1.6 μmol, 4000 eq) was preincubated with 80 μL of 5 mM Cys-MiniAp-4 in water (400 nmol, 1000 eq) to minimize the presence and further formation of peptide dimers linked through a disulfide bond. This solution was mixed with the functionalized QDots and stirred for 1h at room temperature being gently shaken.

Most of the peptide was then removed through a NAP-5 column. To verify the absence of free peptide, the derivatized QDots were buffer-exchanged by centrifugal filtration using a Vivaspin-500 MWCO 100000 (GE Healthcare) until no peptide could be detected by HPLC-UV. The amount of linked peptide was quantified by amino acid analysis after 3-day hydrolysis in 6 M HCl. The last washings were quantified using the same technique and no peptide could be detected.

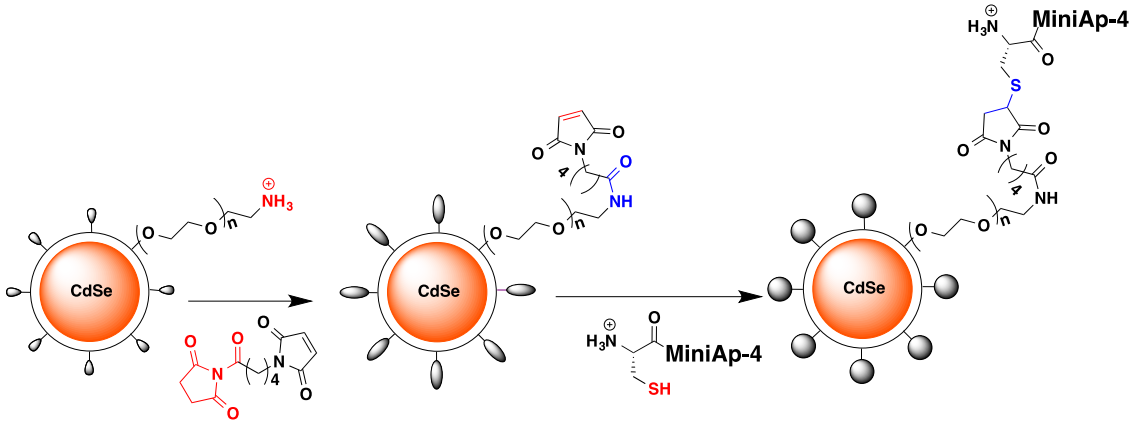

Scheme S3. Scheme of the conjugation of MiniAp-4 to quantum dots.

Gold nanoparticle synthesis and modification. 12 nm AuNPs were synthesized as previously described.[8] Briefly, 50 mL of 1 mM $HAuCl_4$ (Sigma-Aldrich) in water solution was heated at 110 ºC and refluxed for 10 min. 5 mL of 38.8 M sodium citrate was added and the mixture was refluxed for another 30 min. The solution was cooled to room temperature and pH was adjusted to 8.66 with 1M NaOH. Samples were filtered and characterized using a UV-spectrophotometer (Shimazu) and TEM (Tecnai Spirit). Buffer was exchanged through precipitation and resuspension for more diluted 2.2 mM citrate (Sigma-Aldrich). The conjugation was performed by ligand exchange using 8.6 nM AuNPs and 100 μM peptide for 3 h at room temperature under mild shaking. Unconjugated peptide was removed using a PD-10 column (GE Healthcare) and buffer exchange precipitation-resuspension until no peptide was detected by HPLC-UV in the supernatant. Conjugated NPs were again characterized by UV-spectrophotometry and TEM. The amount of conjugated peptide was obtained using amino acid analysis after washing with 1% TFA followed by a 3-day hydrolysis in 6 M HCl. The NPs were quantified spectrophotometrically ($\varepsilon = 5.7 \cdot 10^7\ M^{-1}cm^{-1}$).

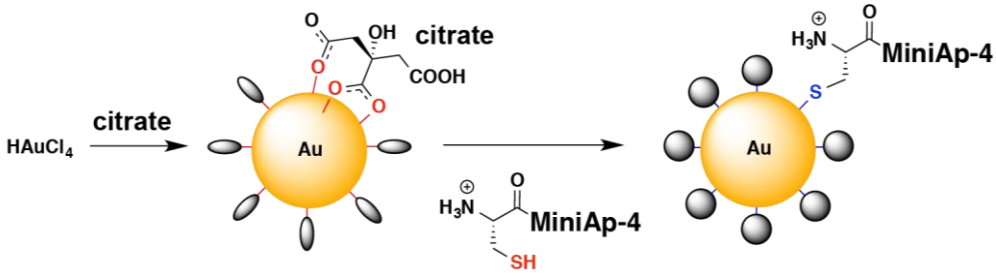

Scheme S4. Scheme of the conjugation of the synthesis of gold nanoparticles and conjugation to MiniAp-4.

Bovine BBB cell-based model assay. This assay was applied as reported by Prades *et al.*[8] Briefly, astrocytes were extracted from 2-5 day Wistar rat pups and bovine brain microvascular endothelial cells (ECCAC BBMVEC B840-05) were subcultured up to passage 3 and frozen. The apical side of 24-well Transwell inserts (Corning) was coated with collagen type IV (Sigma-Aldrich). Then the filters were turned upside down and glial cells (45000 cells/insert) were seeded on the basolateral side of the membrane. Defrosted passage 4-5 bovine endothelial cells were then seeded on the apical side of the Transwell inserts (45000 cells/insert). The co-culture was maintained in EBM2 medium supplemented with bovine brain microvascular endothelial cell growth medium BulletKit (Lonza) and 125 μg/mL of heparin (Sigma-Aldrich); this medium was

changed every 2 days. After 4 days, this it was additionally supplemented with 8-(4-chlorophenylthio)-cAMP and RO-20-1724 (Sigma-Aldrich) and the assay was performed 24 h later. The TEER was measured to control the increasing tightness of the monolayer. Experiments were not initiated until all wells had TEER > 100 ohm·cm^2. It was determined using an ohmmeter Millicell ERS system (MERS 000 01, Millipore) and calculated using the equation (S1):

$$TEER = \left(TEER_{filter\ with\ cells} - TEER_{filter\ without\ cells}\right) \cdot A \qquad \textbf{(S1)}$$

where A is the area of the filter in cm^2

All peptides were assayed at 200 μM in Ringer HEPES. 200 μL of the compound was placed in the apical compartment and 800 μL of plain Ringer HEPES were poured into the basolateral well. After 2 h, the solutions from each compartment were recovered and quantified by HPLC-UV. Lucifer Yellow lithium salt (20 μM) (Sigma-Aldrich) was used as an internal control (Papp < 17·10^{-6} cm/s) and measured in a 96-well plate with a Fluoroskan Ascent Microplate Fluorometer (Thermo Fisher Scientific). Apparent permeability was calculated using equation (S2):

$$P_{app} = \frac{d\ Q_A(t)}{d\ t} \cdot \frac{1}{A} \cdot \frac{V_D}{Q_D(t_0)} \qquad \textbf{(S2)}$$

where P_{app} is obtained in cm/s, t is the length of the assay in seconds, A is the area of the membrane in cm, V_D is the volume in the donor well, $Q_A(t)$ and $Q_{A,Nc}(t)$ are the amounts of compound at time t in the acceptor wells of the plates with and without cells respectively, $Q_D(t_0)$ and $Q_{D,Nc}(t_0)$ are the amounts of compound at the beginning of the experiment in the donor wells of the plates with and without cells respectively.

Human BBB cell-based model assay. This experiment was performed using the model recently developed in the laboratory of Prof. Cecchelli.[9] In brief: Endothelial cells and pericytes were defrosted in gelatin-coated Petri dishes (Corning). Pericytes were cultured in DMEM pH 6.8 while endothelial cells were cultured in supplemented endothelial cell growth medium (Sciencells). After 48 h, pericytes were plated in gelatin-coated 12-well plates (50000 cells/well) and endothelial cells were seeded (80000 cell/well) in 12-well Transwell inserts (Corning) previously coated with Matrigel (Corning). Medium was changed every 2-3 days. Assays were performed 7-8

days after seeding. Lucifer Yellow (50 μM) was used as a control (Papp < $15 \cdot 10^{-6}$ cm/s).

Analyte concentration in the assays was: 200 μM for peptides, 100 nM for ^{125}I labelled GFP constructs, 30 nM for QDot605 and 5 nM for AuNPs. 500 μL of the compound in Ringer HEPES was introduced in the apical compartment and 1500 μL of Ringer HEPES alone in the basolateral compartment. The plates were set on a shaker at 60 rpm (1.6 mm radius) and 37 ºC. After 2 h, the solutions from both compartments were recovered and analyzed. Samples were quantified as follows: an HPLC-UV system for peptides, a gamma counter for ^{125}I labelled GFP and ICP-MS for QDot605 and AuNPs.

Internalization experiments. bEnd.3 cells for internalization and MTT experiments were cultured in DMEM complete medium (glucose 4.5 g/L and 2 mM glutamine) with 10% FBS (both from Sigma). Medium was changed 3 times per week and cells were passaged using 0.05% trypsin/EDTA when they reached 80-90% confluence. For the BBB cell-based models special media were used as specified below. 200000 bEnd.3 cells/well were seeded in 12-well plates. After 2 days of growth, cells were treated with filipin III (10 μg/mL), chlorpromazine (10 μg/mL) or vehicle (Ringer HEPES) for 15 min. After this preincubation time, enough fluorescein-labeled peptide was added to reach a final concentration of 200 μM. After 30 min, cells were washed 5 times with Ringer HEPES at 4 ºC, detached with 0.05% trypsin/EDTA and kept in ice. Cells were immediately analyzed using an FC500-MPL flow cytometer with a 488 nm laser (Beckman Coulter).

Peptide stability in human serum. Peptides at a final concentration of 500 μM were dissolved in HBSS buffer and incubated at 37 ºC in the presence of 90% human serum (from human male AB plasma (Sigma-Aldrich) for 24 h. The 100-μL aliquots extracted at a range of incubation times were treated with 400 μL of MeOH to precipitate serum proteins. After 30 min centrifugation at 13200 *g* and 4ºC, the supernatant was filtered, and MeOH was evaporated at reduced pressure in a SpeedVac instrument. 100 μL of H_2O with 0.1% TFA was added to each sample and they were analyzed by RP-HPLC to calculate the percentage of intact peptide. The samples were also analyzed by MALDI-TOF MS.

Immunogenicity. The immunogenic response of the peptides was evaluated by AntibodyBCN. Free peptides were inoculated to BALB/C mice (n = 4) each other week during 12 weeks. Doses were 25 µg for apamin to avoid toxicity and 50 µg for MiniAp-1 and MiniAp-4 because they did not appear to affect mice in the first immunizations. The first inoculation was performed using Freund's complete adjuvant, while the rest were performed with Freund's incomplete adjuvant. Bleedings from the retromandibular vein were carried out at the beginning (preinoculation) as well as one week after the 4th and the 7th inoculations. The title of antibodies in each bleeding was quantified using an indirect ELISA. Plates were coated with BSA conjugated to each peptide in carbonate buffer (overnight at 4ºC) and subsequently blocked with powder milk (2 h at 37 ºC). Serial dilutions (1/2) starting in 1/100 were incubated (1 h at 37 ºC). Anti-mouse IgG-HRP (Acris) was used as a detection antibody (1/5000 dilution, 1 h at 37 ºC). Colorimetric quantification was achieved adding TMB (100 µL, 30 min), which was stopped with 1 M HCl (100 µL), and reading the plate at 450 nm. An IC50 was calculated when absorbance saturation was reached under these conditions.

Other experiments performed on animals. 5-week CD1 mice (*Mus musculus*) were obtained from Charles River. Animals were housed at the Barcelona Science Park or in the Hospital Clinic de Barcelona animal facility in a 12 h light/dark cycle according to the standard of holding facility and were fed ad libitum. All experiments were approved by the animal ethics committee of the Barcelona Science Park or the Hospital Clinic de Barcelona respectively.

Single-dose acute toxicity test. 4 groups (n = 6) of male mice were used (20 ± 2 g). Each group was injected with 200 µL of one of the following solutions: MiniAp-1 (1200 nmol, roughly the solubility limit) or MiniAp-4 solutions (1200 nmol), 0.25 mM apamin solution (200 nmol) or sterile water. Mice were observed during the first hour and after 2, 4, 8 and 24 h.

In vivo total animal fluorescence imaging. Cyanine5.5 conjugates were injected via the tail vein (4 nmol in 150 µL of sterile water) in 6- to 7-week-old CD1 male mice (n = 4). Fluorescence was measured in an IVIS Spectrum Pre-clinical In Vivo Imaging System (IVIS-200) 0.5, 1, 2, 4, 8 and 24 h after injection. Filters were set to measure cyanine5.5 subtracting cyanine5.5 background (1-s exposure). The heads of the animals

were shaved before the first measurement, and for each time-point mice were anesthetized with isofluorane for 3 min and kept under anesthesia during image acquisition. Between measurements, mice were allowed to recover and were fed *ad libitum*. Three groups of mice (n = 4) were injected either with cyanine5.5-MiniAp-4, cyanine5.5-cysteamine or vehicle (sterile water). Net photon flux calculated by subtracting the flux from the group injected with the vehicle and AUC are given.

Ex vivo fluorescence imaging. Cyanine5.5 conjugates were injected via the tail vein (4 nmol in 150 µL of sterile water) in 6- to 7-week-old CD1 male mice (n = 4). After 1 h, mice were deeply anesthetized, imaged in the IVIS chamber and perfused with PBS for 5 min. Subsequently, mice were killed and the organs were immediately excised and the fluorescence was quantified in the IVIS chamber.

Preparation and microscopy imaging of brain slices. Cyanine5.5 conjugates were injected via the tail vein (4 nmol in 150 µL of sterile water) in 6- to 7-week-old CD1 male mice (n = 3). After 1h, animals were deeply anesthetized and perfused with PBS followed by PFA to fix the tissues and the molecules for microscopy. Brains were immerged in sucrose 30% until density was equaled inside the tissue and cryoprotected with OTC before freezing. Tissues were cut in coronal 15 or 50 µm slices using a cryostat. Frozen sections were permeabilized with PBS bearing 0.3% Triton X-100 (PBST) and treated with blocking solution (PBS containing 5% goat serum in PBST). In 50 µm slices capillaries were stained by free-floating with lectin-rhodamine for 2 h (1:500, Vector Labs). In 15 µm slices neurons were stained overnight with rabbit anti-NeuN antibody (1:100; Abcam) and glial cells with rabbit anti-GFAP (1:200; Abcam). After washing with PBST, the secondary antibody used was goat anti-rabbit Alexa 488 (1:500; Abcam). Antifading fluorescence mounting medium (Dako) was used to mount the slides. Samples were visualized in a Leica TCS SP5 MP system (DMI 6000) inverted spectral confocal microscope. A 63x/1.3 glycerol and a 20x/0.75 objectives were used.

Statistical analysis. Unpaired two-tailed student *t* tests were applied to evaluate the significant difference or *p* values between data sets using Prism 6.0c software.

Supplementary results and figures

Peptide characterization - HPLC and MS. Yields were calculated after purification and quantification by amino acid analysis. * = yield of the fluorophore-peptide conjugation step.

HPLC or UPLC chromatograms and MALDI-TOF or LC-ESI-Q mass spectra are shown for each synthesized peptide. All HPLC chromatograms here shown were recorded at 220 nm in an 8-min linear gradient from 0 to 100% of MeCN with (0.036% TFA) in H_2O (0.045% TFA) unless otherwise specified. All U-HPLC chromatograms here shown were recorded at 220 nm in a 2-min linear gradient from 0 to 100% of MeCN with (0.036% TFA) in H_2O (0.045% TFA). Values displayed on the chromatograms represent time in minutes and those on the mass spectra correspond to the observed $[M+H]^+$. UPLC t_R and LC-ESI-Q m/z are shown in italics to distinguish them from HPLC t_R and MALDI-TOF, respectively.

For the nomenclature of cyclic peptides we followed the abbreviation rules proposed by Spengler *et al.*[10]

Table S1. Properties, purity and yield of the peptides used in this study.

Peptides	Calc Mw	FTMS Mw	$[M+H]^+$ MALDI-TOF MS	t_R HPLC, min	Purity, %	Yield, %	Sequence, cargoes and linkers
Apamin	2025.887	2025.882	2027.0	3.4	> 99	8	C(&^{1})NC(&^{2})KAPETALC(&^{1})ARRC(&^{2})QQH-NH_2
MiniAp-1	1599.641	1599.640	1600.8	3.9	95	5	C(&^{1})NC(&^{2})KAPETALC(&^{1})AAAC(&^{2})H-NH_2
MiniAp-2	727.423	727.423	728.5	3.5	> 99	30	KAPETAL-NH2
MiniAp-3	931.426	931.427	932.5	*3.8*	> 99	10	C(&)KAPETALC(&)-NH2
MiniAp-4	910.487	910.487	911.5	3.7	99	12	[Dap](&)KAPETALD(&)-NH_2
MiniAp1-β_sheet_breaker-peptide	2276.971	2276.973	2277.1	5.0	> 99	5	C(&^{1})NC(&^{2})KAPETALC(&^{1})AAAC(&^{2})-HLPFFD-NH2
cFluorescein-MiniAp-1	1957.689	1957.690	1959.0	4.9	92	2	carboxyfluorescein-C(&1)NC(&2)KAPETALC(&1)AAAC(&2)H-NH2
cFluorescein-MiniAp-4	1325.556	1325.561	1326.7	4.6	98	7	carboxyfluorescein-G[Dap](&)KAPETALD(&)-NH_2
levodopa-MiniAp-1	1778.700	1778.699	1780.1	3.9	> 99	1	levodopa-C(&1)NC(&2)KAPETALC(&1)AAAC(&2)H-NH2
levodopa-MiniAp-4	1089.546	-	1090.7	3.7	> 99	6	levodopa-[Dap](&)KAPETALD(&)-NH2
sRhodamine-MiniAp-1	2197.810	2197.821	2197.8	5.1	91	0.2	sulforhodamineB-C(&1)NC(&2)KAPETALC(&1)AAAC(&2)H-NH2
cyanine5.5-cysteamine	781.403	781.405	*783.3*	*1.98*	> 99	51*	cyanine5.5-cysteamine
cyanine5.5-MiniAp-4	1717.869	1717.877	1718.9	*1.88*	> 99	48*	cyanine5.5-[Dap](&)KAPETALD(&)-NH_2
maleimide-MiniAp-4	1103.561	1103.560	1104.5	4.2	> 99	4	maleimidohexanoyl-[Dap](&)KAPETALD(&)-NH2
maleimide-MiniAp-4(scram)	1103.560	1103.560	1104.8	*1.37*	93	5	H-C[Dap](&)LTAKEPAD(&)-NH_2
Cys-MiniAp-4	1013.496	*1013.498*	1014.6	3.9	> 99	4	H-C[Dap](&)KAPETALD(&)-NH_2

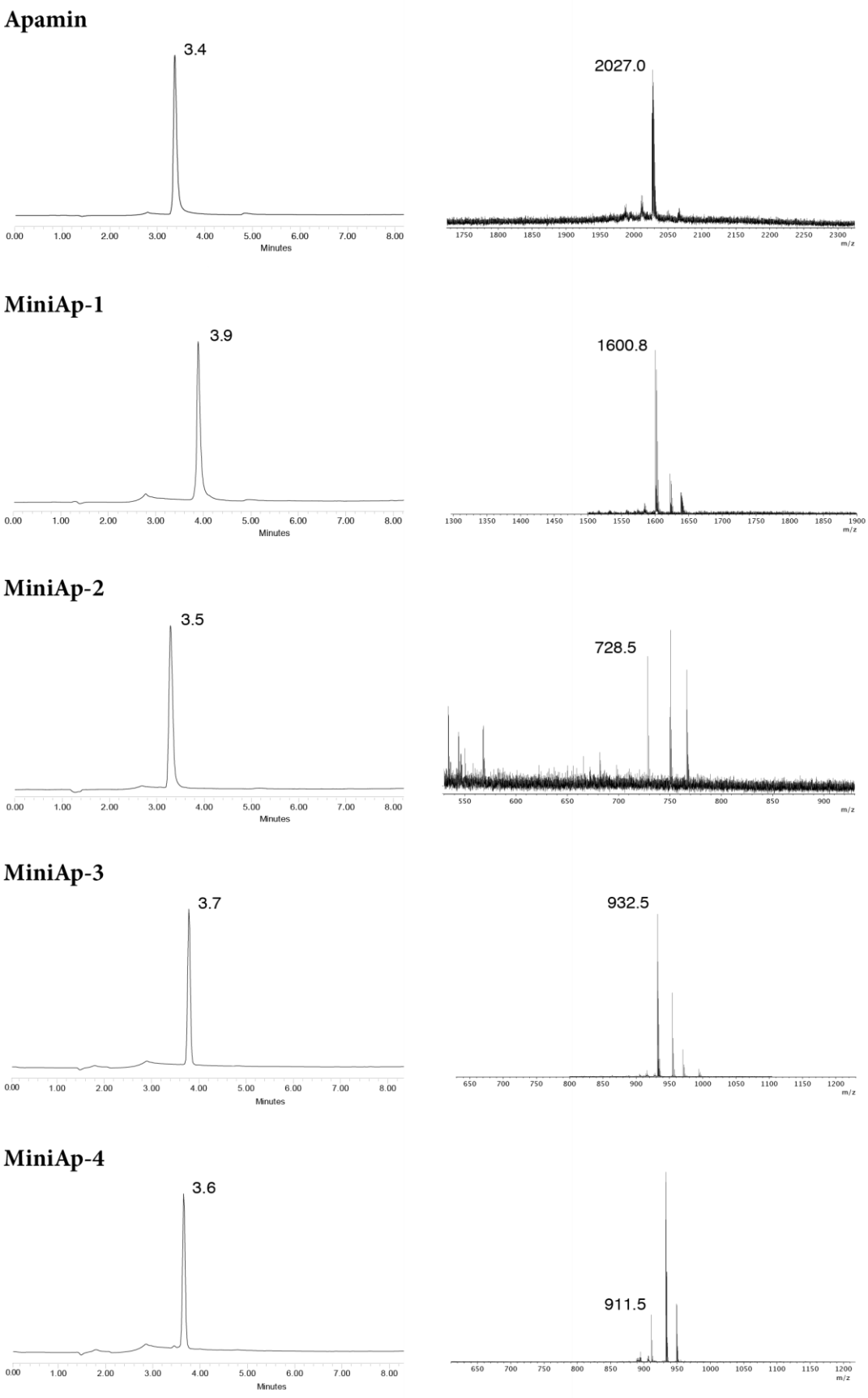

Figure S1 (continued in the following page.). HPLC traces and MS spectra of all peptides used in this study.

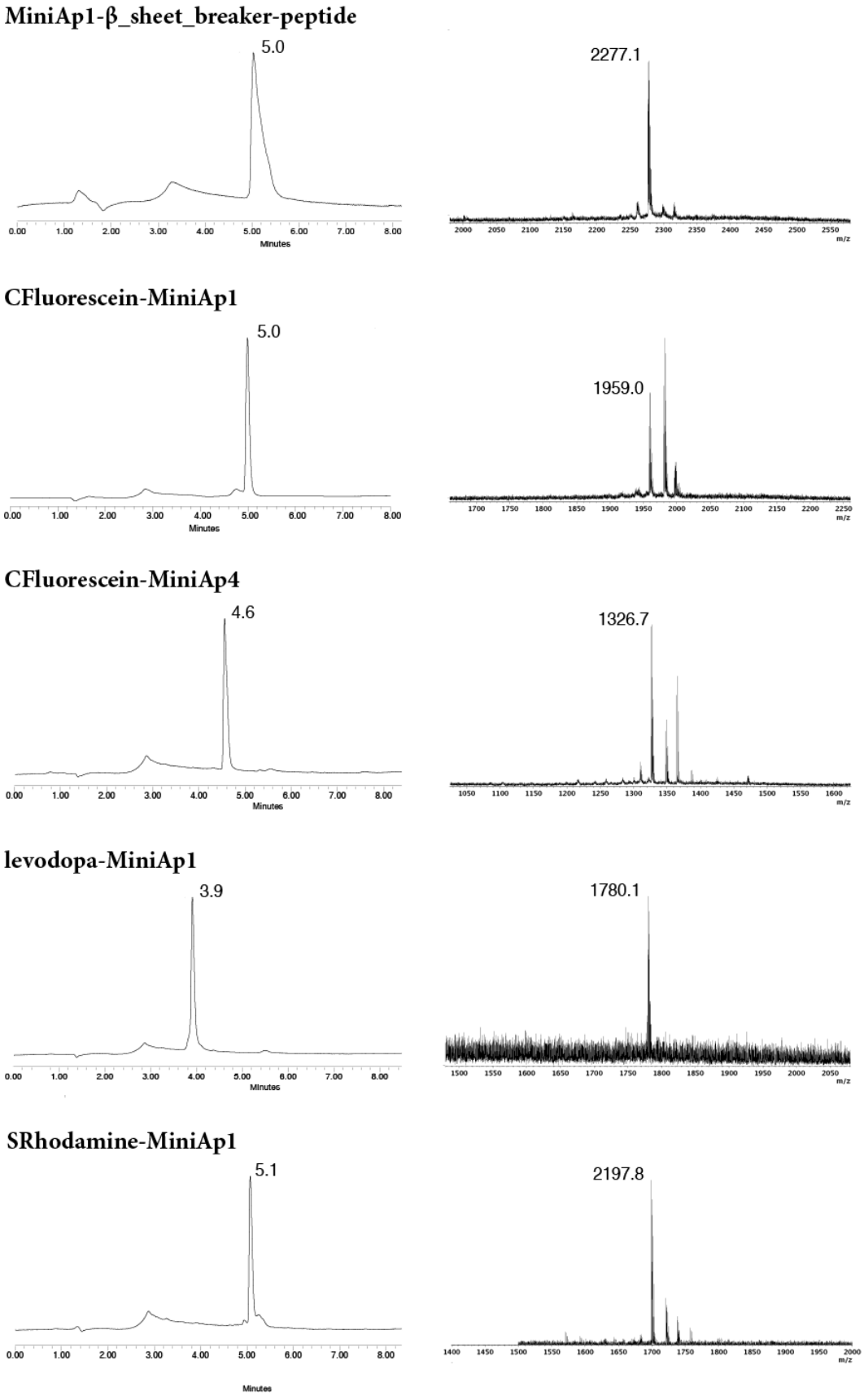

Figure S1 (continued from the previous page and in the following page.). HPLC traces and MS spectra of all peptides used in this study.

cyanine5.5-cysteamine

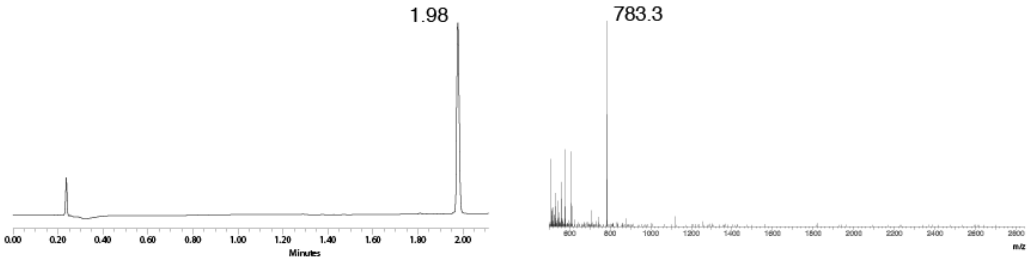

cyanine5.5-MiniAp4

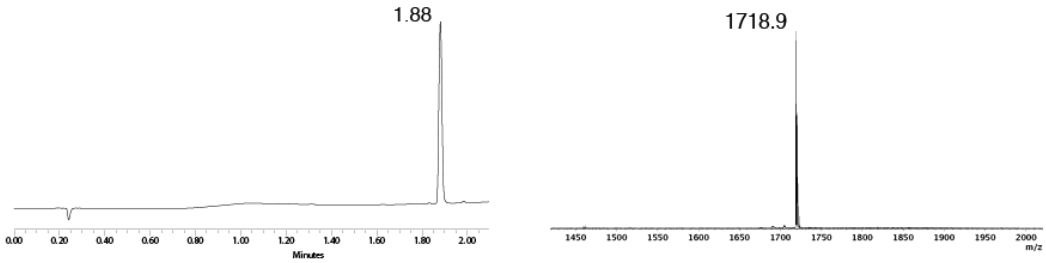

cyanine5.5-THR

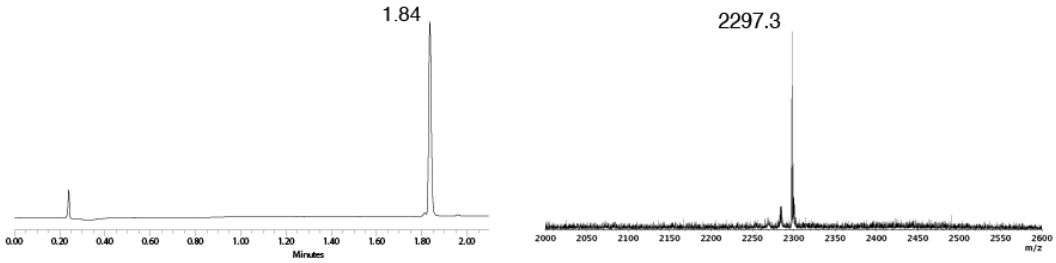

maleimide-MiniAp4

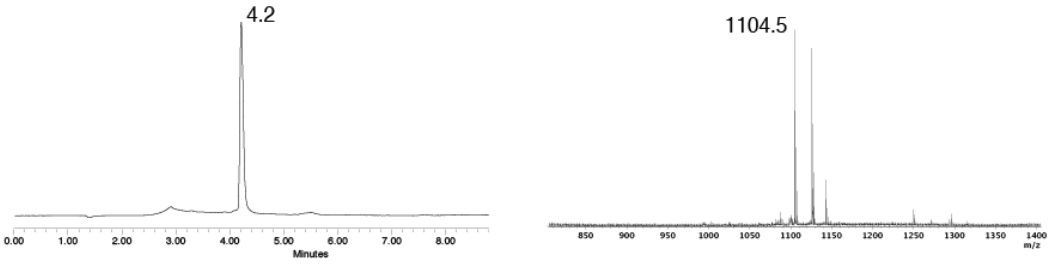

maleimide-MiniAp4(scram)

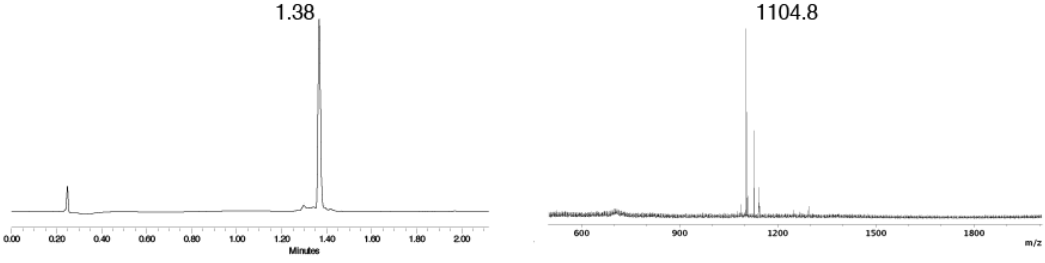

Figure S1 (continued from the previous page and in the following page.). HPLC traces and MS spectra of all peptides used in this study.

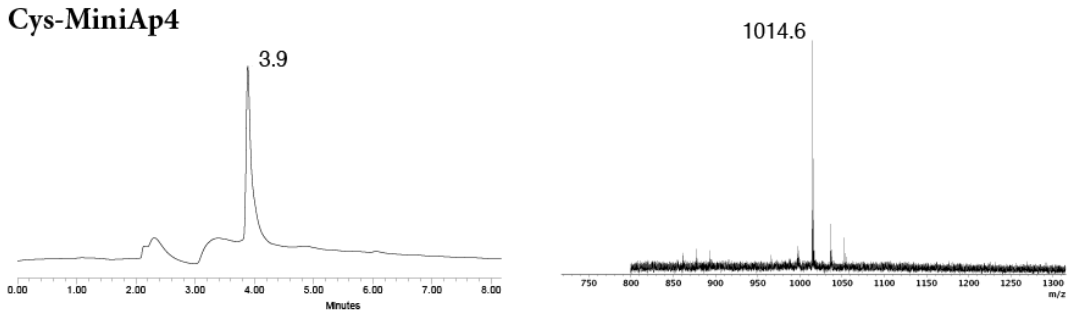

Figure S1 (continued from the previous page.). HPLC traces and MS spectra of all peptides used in this study.

Permeability and internalization of peptides in cell-based models

Table S2. Permeability of peptides assayed in the bovine cell-based BBB model.

Peptide	Treatment	Normalized Papp*	SD
Ap	-	0.62	0.08
MiniAp-1	-	1.00	0.08
MiniAp-1	4ºC	0.19	0.03
MiniAp-1	basal-apical	0.66	0.02
MiniAp-1	NaN_3	0.58	0.06
Ld-MiniAp-1	-	0.96	0.11
Cf-MiniAp-1	-	0.85	0.30
SrG-MiniAp-1	-	0.74	0.11
MiniAp-1-Lp	-	0.85	0.19
MiniAp-2	-	0.74	0.22
MiniAp-3	-	0.96	0.17
MiniAp-4	-	1.49	0.14
MiniAp-4	Chlorpromazine	1.42	0.13
MiniAp-4	Filipin III	0.76	0.04
Angiopep-2	-	0.85	0.08

*The Papp of all peptides was normalized by the Papp of MiniAp-1: $(2.6 \pm 0.3)\cdot 10^{-6}$ cm/s, which was always assayed as a control. In the human cell-based BBB model the permeability of MiniAp-4 was $6.7 \pm 0.6)\cdot 10^{-6}$ cm/s.

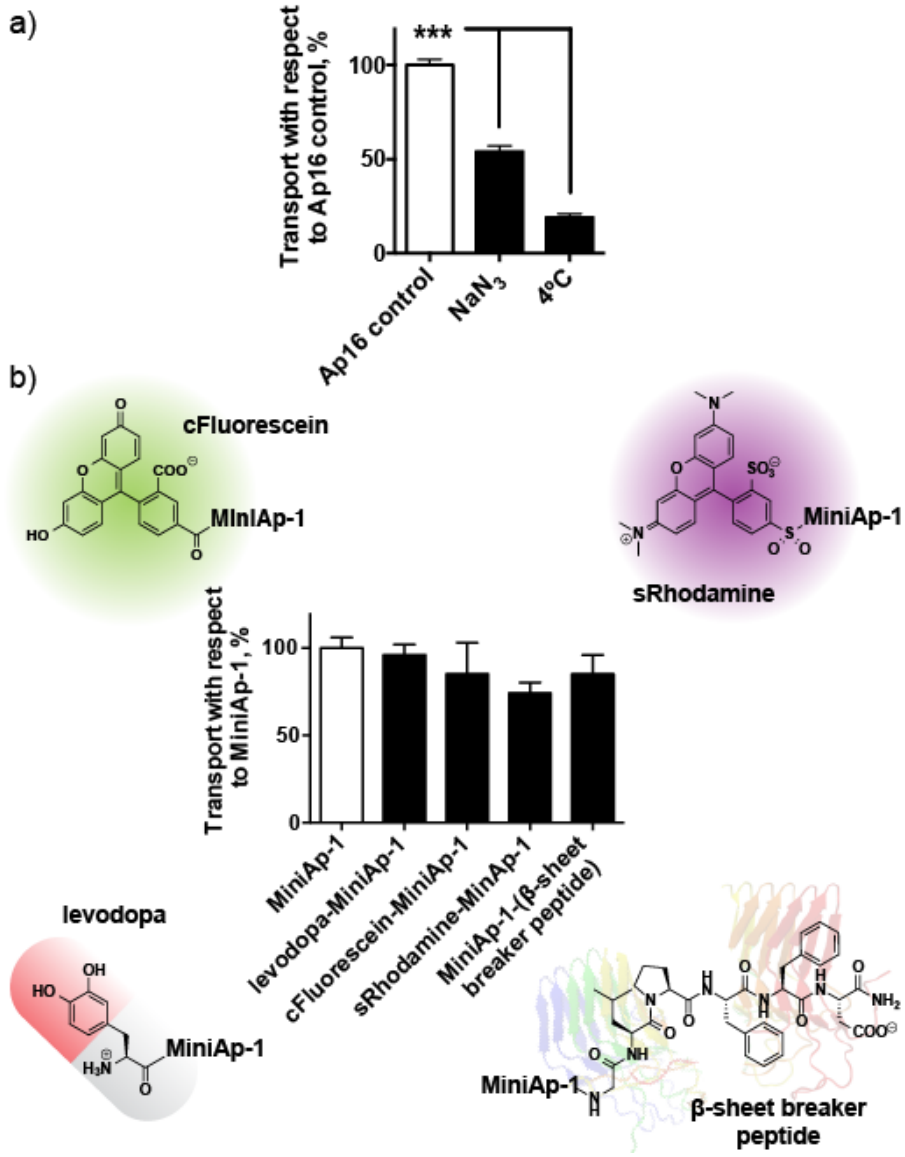

Figure S2. MiniAp-1 is a good BBB-shuttle candidate as it is transported by an active mechanism and is able to carry small cargoes across a tight monolayer of endothelial cells. a) Effect of reverse transport (basal to apical), sodium azide and low temperature on the permeability of MiniAp-1 in a bovine BBB cell-based model. b) Effect of the conjugation of small cargoes to MiniAp-1 permeability in the same model. The amyloid amyloid β-sheet breaker peptide had been described by Soto *et al.*[11] All values are reported as the mean ± SEM ($n = 3$, *** $p < 0.001$).

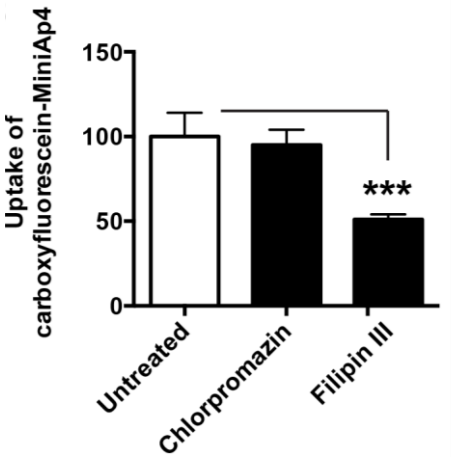

Figure S3. Effect of selective inhibitors on the uptake of CFluorescein-MiniAp4 by bEnd.3 cells analysed by FACS. All values are reported as the mean ± SEM ($n = 3$, *** $p < 0.001$).

NMR

Two distinct sets of resonances were observed in the ^{1}H NMR spectrum of MiniAp-1 with relative populations of 90% and 10%. The minor species was identified as the *cis* Pro conformer on the basis of strong $d_{\alpha\alpha}$(Ala-5/Pro-6) NOE and the Pro C_β - C_γ chemical shift difference ($\Delta\delta$ = 9.2 ppm).[12] The chemical shift differences between the Pro6 C_β and C_γ atoms (4.4 ppm) and the characteristic sequential NOE observed between the H_α of Ala-5 and the H_δ of Pro-6 confirmed that, as previously observed for apamin, the *trans* rotamer was the major MiniAp-1 species. Structural characterization of the *trans* conformer was done on the basis of NMR parameters such as H_α and $^{13}C_\alpha$ secondary chemical shifts, temperature coefficients of NH amide protons and NOEs. The ^{1}H chemical shifts (Table S3) and the overall pattern of NOEs (Fig. S5A) of the trans MiniAp-1 isomer were very similar to those described for the native peptide, suggesting that both compounds adopt a similar conformation in solution. Consecutive deviations from random coil values, negative for H_α and positive for $^{13}C_\alpha$ (Fig. S5B), were observed for the Ala-9-His-16 MiniAp-1 segment, clearly indicating a helical fold in this region. The presence of $d_{NN}(i,i+1)$, $d_{\alpha N}(i,i+3)$, $d_{\alpha N}(i,i+4)$ and $d_{\alpha\beta}(i,i+3)$ NOEs in the Thr-8-Cys-15 segment was also diagnostic of a regular α–helix. The observation of several non-sequential NOEs at the *N*-terminus and of medium-strong $d_{NN}(i,i+1)$ NOEs between Cys-3 and Lys-4 and between Lys-4 and Ala-5 is consistent with a change of backbone direction indicative of a turn-like structure, as previously described for apamin. Temperature coefficients and $^{3}J_{\alpha N}$ coupling constants (Table S4) also support the chemical shift- and NOE-based conformational analysis.

To obtain the three-dimensional structure of MiniAp-1, we conducted a simulated annealing calculation by applying distance and dihedral angle constraints as described in the Methods section. An overlay of the ten lowest-energy structures from the calculation is shown in Figure S4. The structure of MiniAp-1 consists of an *N*-terminal loop (residues 1-8) and a *C*-terminal α-helix (residues 9-15), which is very similar to that of apamin,[13] with a rmsd value of 0.72 Å for the backbone superposition of both structures. However they display some local differences in the loop orientation and in the *C*-terminal residue which is less defined in the Miniap-1 structure.

MiniAp-2 did not show any evidence of α-helical formation in terms of H_α and C_α chemical shifts deviations, NOE connectivities, $^3J_{\alpha N}$ coupling constants and temperature coefficients of amide protons (Table S4).

Notably, the NMR spectra of both Miniap-3 and Miniap-4 showed equally populated *cis* and trans conformers. The *cis-trans* species were identified on the basis of strong $d_{\alpha\delta}$ (Ala-5/Pro-6) NOEs in the case of the *trans* and $d_{\alpha\alpha}$ (Ala-5/Pro-6) NOEs in the case of the *cis* rotamer. This observation was further confirmed by the chemical shift difference between the Pro-6 C_β and C_γ atoms: *trans*-Pro C_β-C_γ ($\Delta\delta$ = 4.5 for both MiniAp-3 and MiniAp-4) and *cis*-Pro C_β-C_γ ($\Delta\delta$ = 9.2, for both MiniAp-3 and MiniAp-4).

The close resemblance of H_α and C_α chemical shifts (Table S3), $^3J_{\alpha N}$ coupling constants and NH temperature coefficients (Table S4) between the *trans* conformers of both peptides on one side and between the *cis* conformers on the other side, suggested that the backbone conformation adopted for MiniAp-3 and MiniAp-4 are very similar. The above-mentioned NMR parameters did not suggest a defined secondary structure for either the *cis* or the *trans* conformers of both monocyclic derivatives. In addition, in the NOESY spectra of both analogues only sequential NOE connectivities were observed, implying that these peptides do not exhibit any dominant secondary structure. These results were also consistent with the CD spectra obtained for these analogues which were very similar to that of the MiniAp-2. However, when compared to the linear peptide, the trans conformers of both monocyclic derivatives showed significantly larger amide chemical shift dispersion (Figure 3), suggesting less conformational flexibility. Significant differences in $^{13}C_\alpha$ chemical shifts were also observed between each conformer of both monocyclic derivatives and the linear MiniAp-2 peptide, further suggesting that cyclization constrains the peptide (Figure 3).

Interestingly, the temperature coefficients ($-\Delta\delta/\Delta T$) of Thr^6 NH were 0.5 and 2.5 ppb/K for *trans* MiniAp-3 and *trans* MiniAp-4, respectively, suggesting that this amide proton may be involved in an intramolecular hydrogen bond in the conformation adopted by the *trans* conformers. In contrast, the higher temperature dependence of the Thr-6 NH

chemical shift in the *cis* conformers, $-\Delta\delta/\Delta T$ = 9.0 (*cis* MiniAp-3) and 7.5 ppb/K (*cis* MiniAp-4) was indicative of a solvent exposed amide.

Table S3. ^{1}H-NMR chemical shifts (ppm) of the apamin analogs: (A) *trans* MiniAp-1, (B) *trans* MiniAp-2, (C) *trans* MiniAp-3, (D) *cis* MiniAp-3, (E) *trans* MiniAp-4, (F) *cis* MiniAp-4.

	NH						αCH						βCH					
Residue	A	B	C	D	E	F	A	B	C	D	E	F	A	B	C	D	E	F
Cys							4.44						3.13					
													2.73					
Asn	9.27						4.90						3.08					
													2.78					
Cys/Dapa	9.09						4.70		4.36	4.32	4.21	4.24	3.31		3.41	3.33	3.81	3.86
													2.77		3.31	3.15	3.70	3.50
Lys	8.06		8.92	8.63	8.80	8.68	4.25	4.00	4.37	4.43	4.24	4.42	1.84	1.90	1.88	1.84	1.87	1.85
															1.77	1.75	1.80	1.75
Ala	7.28	8.75	7.81	8.48	8.15	8.49	4.56	4.63	4.68	4.32	4.66	4.27	1.20	1.40	1.37	1.36	1.38	1.36
Pro							4.47	4.44	4.39	4.63	4.42	4.65	2.00	2.32	2.33	2.28	2.31	2.30
													1.78	1.92	1.98	2.16	1.96	2.28
Glu	9.16	8.48	7.86	8.66	8.00	8.70	4.30	4.40	4.43	4.47	4.41	4.50	2.27	2.13	2.24	2.21	2.23	2.20
													2.16	2.01	2.06	2.14	2.05	2.12
Thr	7.61	8.15	8.02	8.02	7.98	7.98	4.66	4.30	4.25	4.30	4.17	4.23	4.62	4.19	4.25	4.33	4.22	4.30
Ala	8.99	8.36	8.53	8.39	8.53	8.27	4.19	4.34	4.26	4.24	4.24	4.24	1.48	1.39	1.42	1.43	1.41	1.40
Leu	8.22	8.18	7.83	8.00	7.83	7.99	4.17	4.28	4.34	4.31	4.34	4.28	1.70	1.59	1.71	1.63	1.63	1.62
													1.57	1.65	1.64			
Cys/Asp	7.81		8.02	8.02	7.97	7.99	4.70		4.61	4.60	4.70	4.73	3.18		3.28	3.37	2.88	2.87
													2.81		3.19	3.15	2.77	2.76
Ala	8.45						3.78						1.45					
Ala	7.89						4.15						1.50					
Ala	7.94						4.19						1.57					
Cys	8.11						4.44						3.00					
													2.90					
His	7.83						4.62						3.39					
													3.27					

Table S3 (continued from the previous page)

Residue	others					
	A	B	C	D	E	F
Cys						
Asn	NH_2 7.07, 7.68				NH 8.26	NH 8.24
Cys/Dapa						
Lys	γCH_2 1.43, 1.52	γCH2 1.47	γCH_2 1.43	γCH_2 1.46	γCH_2 1.46	γCH_2 1.46
	δCH_2 1.69	δCH_2 1.70	δCH_2 1.68	δCH_2 1.69	δCH_2 1.69	δCH_2 1.69
	εCH_2 3.00	εCH_2 3.02	εCH_2 3.00	εCH_2 3.01	εCH_2 3.00	εCH_2 3.01
	εNH_3 7.53	εNH_3 7.54	εNH_3 7.52	εNH_3 7.52	εNH_3 7.53	εNH_3 7.53
Ala						
Pro	γCH_2 2.11, 2.00	γCH_2 2.04	γCH_2 2.02	γCH_2 1.98, 1.81	γCH_2 2.02	γCH_2 1.98, 1.80
	δCH_2 3.57, 3.47	δCH_2 3.83, 3.68	δCH_2 3.73, 3.67	δCH_2 3.56, 3.53	δCH_2 3.78, 3.67	δCH_2 3.55
Glu	γCH_2 2.60	γCH_2 2.51	γCH_2 2.47	γCH_2 2.52	γCH_2 2.48	γCH_2 2.49
Thr	γCH_2 1.26	γCH_2 1.21	γCH_2 1.24	γCH_2 1.19	γCH_2 1.24	γCH_2 1.18
Ala						
Leu	γCH_2 1.70	γCH_2 1.65	γCH_2 1.63	γCH_2 1.65	γCH_2 1.62, 1.58	γCH_2 1.62
	δCH_3 0.95, 0.89	δCH_3 0.93, 0.87	δCH_3 0.95, 0.89	δCH_3 0.94, 0.89	δCH_3 0.92, 0.87	δCH_3 0.93, 0.87
Cys/Asp						
Ala						
Ala						
Ala						
Cys						
His	C_2H 8.62					
	C_4H 7.35					

Table S4. $^{3}J_{\alpha}N$ coupling constants and temperature coefficient values obtained for the apamin analogs: (A) trans MiniAp-1, (B) trans MiniAp-2, (C) trans MiniAp-3, (D) cis MiniAp-3, (E) trans MiniAp-4, (F) cis MiniAp-4. ov. and b.s. indicate overlap and broad signal, respectively.

	$^{3}J\alpha N$ (Hz)						-Δδ/ΔT (ppb/K)					
Residue	A	B	C	D	E	F	A	B	C	D	E	F
Cys												
Asn	9.2						4.0					
Cys/Dapa	5.3						8.5					
Lys	8.1		6.9	7.5	5.9	7.3	1.5		5.0	6.0	5.0	6.0
Ala	7.5	5.1	7.1	4.9	6.5	4.5	2.0	7.0	7.0	8.0	6.5	8.5
Pro												
Glu	6.5	6.7	7.7	6.5	ov.	6.7	7.5	9.0	13.5	5.0	8.5	4.0
Thr	b.s.	7.5	7.1	7.9	5.9	7.8	3.0	8.0	0.5	9.0	2.5	7.5
Ala	3.5	6.0	4.9	5.0	4.8	ov.	5.5	9.0	5.5	6.0	7.0	4.5
Leu	4.5	7.1	7.5	ov.	7.4	ov.	8.0	9.0	8.0	7.5	7.5	9.5
Cys/Asp	6.1		7.7	7.4	7.5	ov.	4.5		6.5	5.0	5.0	8.5
Ala	3.8						4.0					
Ala	5.0						4.0					
Ala	5.0						3.0					
Cys	6.1						4.5					
His	7.2						1.5					

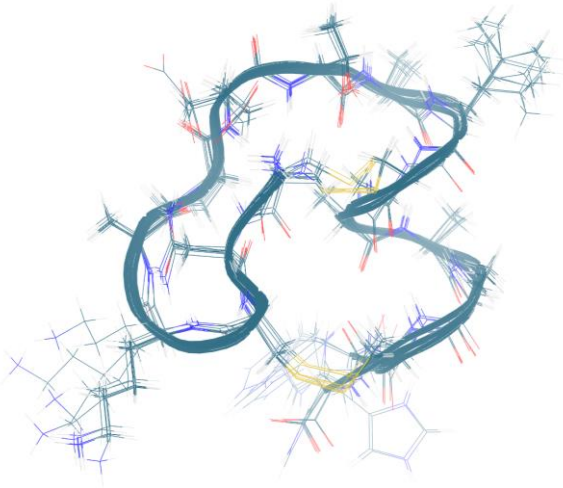

Figure S4. Ensemble of the best 10 structures of MiniAp-1. Root-mean-square deviation (RMSD) values of 0.24 and 1.31 Å were calculated for the backbone and heavy atom superimposition respectively. The main features of MiniAp-1 structure are the same as those of apamin, i.e. an *N*-terminal loop (residues 1-8) and a *C*-terminal α-helix,[13] with a RMSD value of 0.72 Å for the backbone superposition of both structures. Only the loop orientation is slightly different and the *C*-terminal residue is less defined in MiniAp-1.

Table S5. MiniAp-1 3D structure statistics.

Restraints	
NOE	
Sequential ($\|i-j\| = 1$)	21
Medium range ($1 < \|i-j\| \leq 4$)	25
Long range ($\|i-j\| > 4$)	6
Dihedral angle	
ϕ	8
ψ	8
Ramachandran	
Most favoured regions	12 (92.3%)
Additional allowed regions	1
Generously allowed regions	0 (0%)
Disallowed regions	0 (0%)

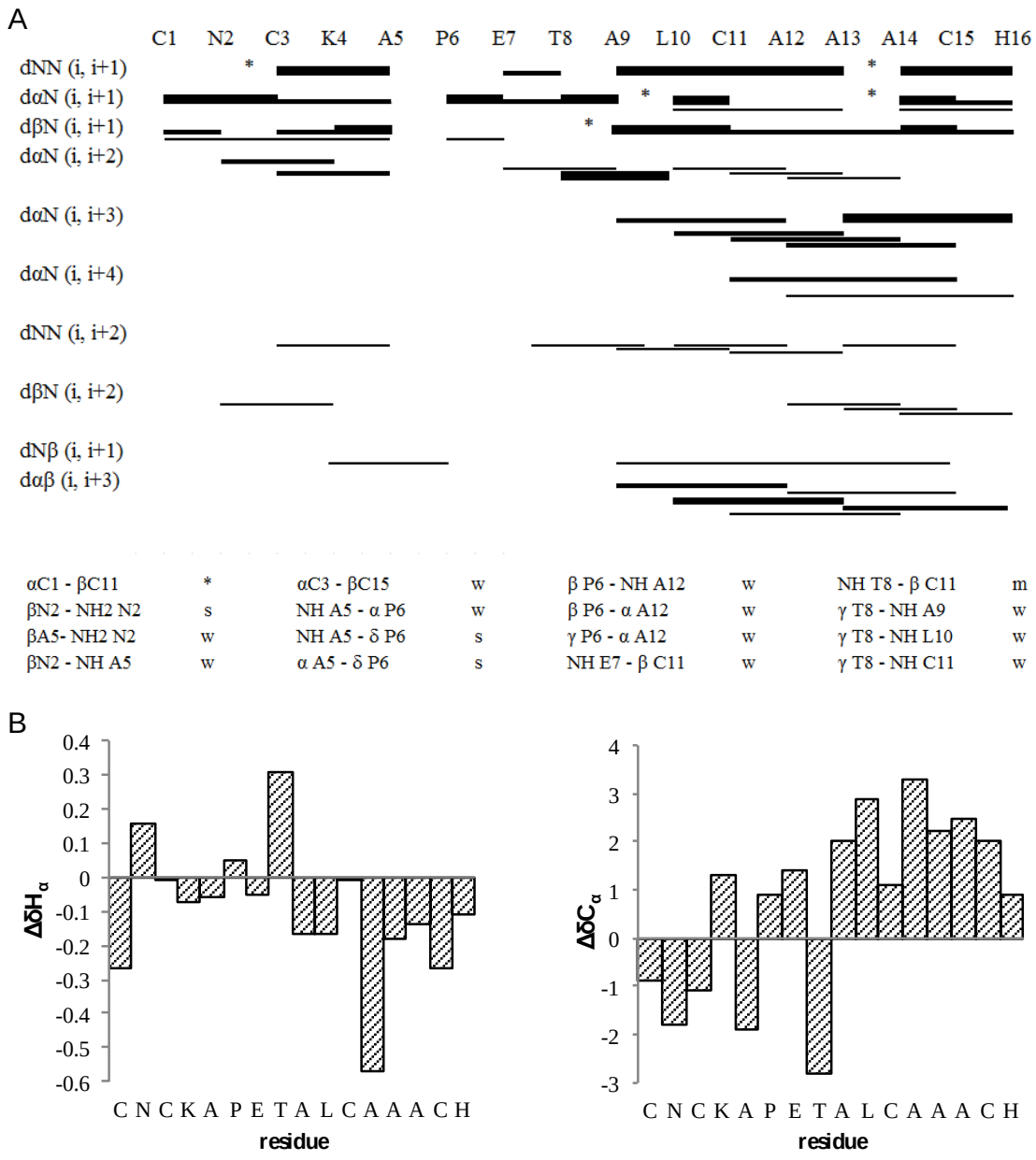

Figure S5. A) Summary of NOE connectivities observed for MiniAp-1 (mixing time 250 ms). The thickness of the bar indicates the strength of the NOE (weak, medium or strong). The stars indicate signal overlap. B) Deviations of trans MiniAp-1 ^{1}Hα (left) and ^{13}Cα (right) chemical shift values from random coil values.[14] $\Delta\delta = \delta_{observed} - \delta_{random}$.

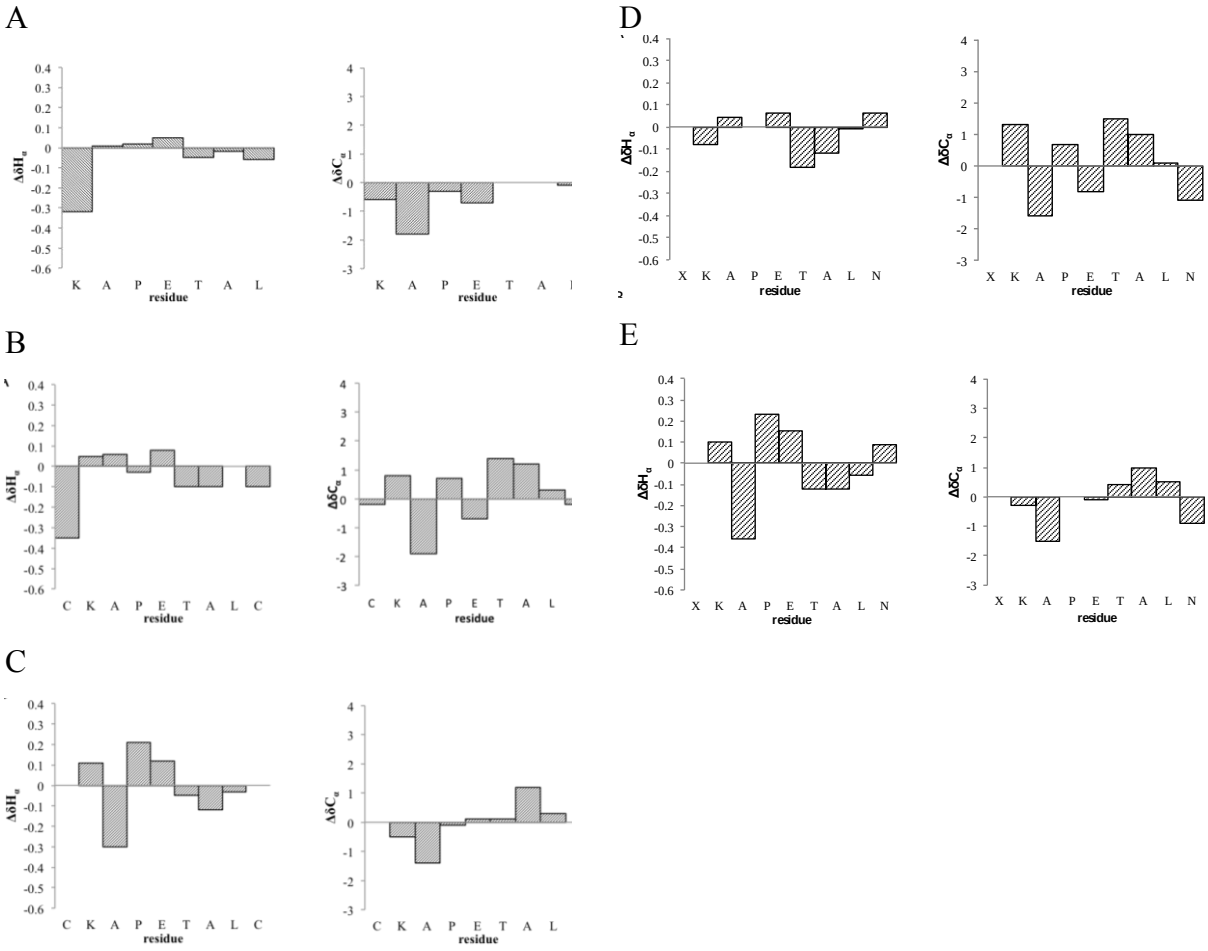

Figure S6. Deviations from random coil values[14] (Δδ = δobserved - δrandom) of 1Hα (left) and 13Cα (right) chemical shifts for: A) MiniAp-2. B) *trans* MiniAp-3. C) *cis* MiniAp-3. D) *trans* MiniAp-4. E) *cis* MiniAp-4.

MiniAp-4 conjugate characterization

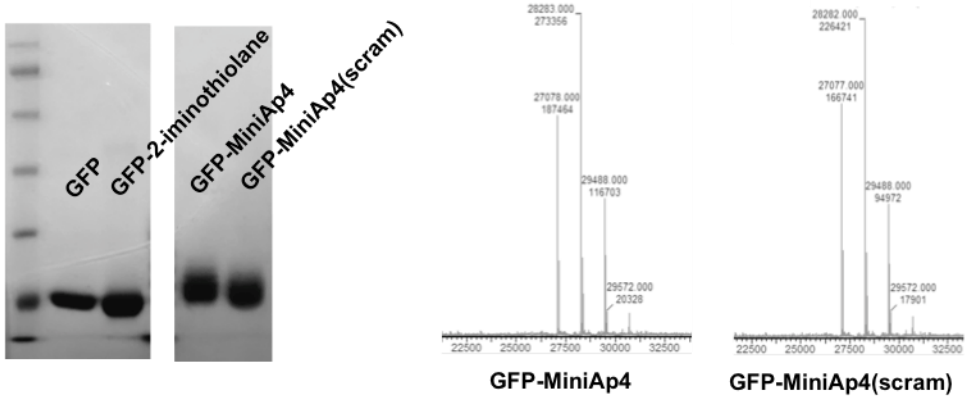

Figure S7. Characterization of GFP-MiniAp-4. Coomassie-stained SDS-PAGE (left) and LC-MS deconvoluted spectrum (right):

Table S6. Mass corresponding to the species obtained upon conjugation of GFP.

# peptides	Expected	Found	
		MiniAp-4	MiniAp-4(scram)
0	27096	27078	27077
1	28301	28283	28282
2	29506	29488	29488
3	30711	30694	30694

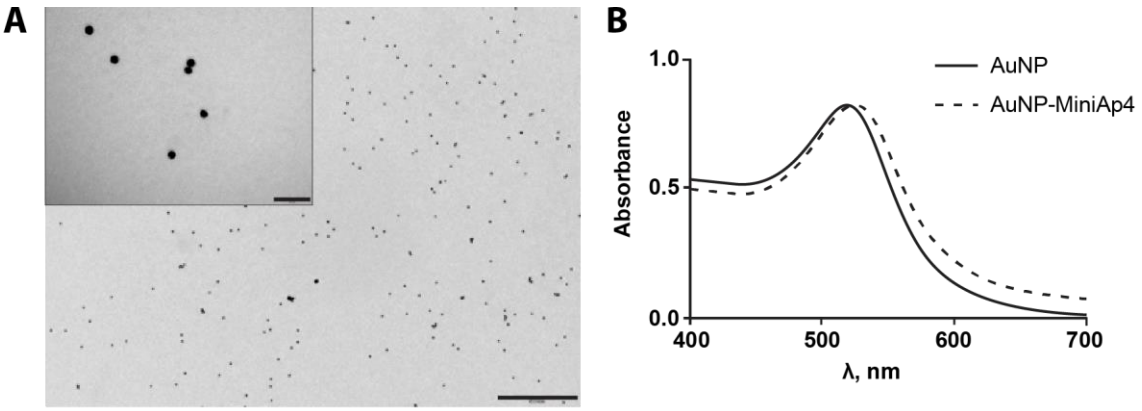

Figure S8. Synthesized and conjugated AuNPs. A) TEM micrographies. Scale bars: 500 nm in the low magnificaiton image and 50 nm in the zoomed image. B) Absorption spectra.

Permeability and internalization of MiniAp-4 conjugates in cell-based models

Table S7. Permeability of large cargoes and cargo-BBB-shuttle constructs in the human cell-based BBB model.

Construct	P_{app}, $\cdot 10^{-7}$ cm/s	SD
GFP	7.5	1.5
GFP-MiniAp-4(scrambled)	7.0	0.7
GFP-MiniAp-4	11.9	0.16
QD	0.82	0.26
QD-MiniAp-4	1.63	0.1
AuNP	< 0.01**	
AuNP-MiniAp-4	0.20	0.02

** Quantification limit

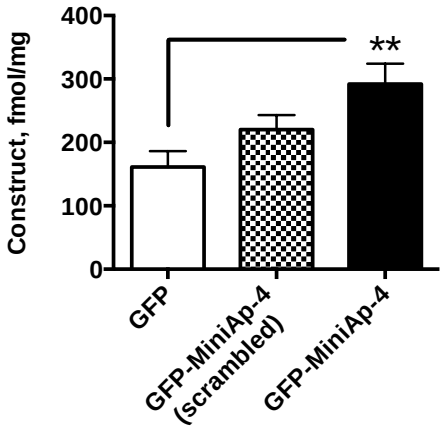

Figure S9. In contrast to GFP-MiniAp-4(scrambled), GFP-MiniAp-4 is internalized more efficiently than GFP by bEnd.3 cells. ** $P < 0.01$ (t-test).

In vivo experiments

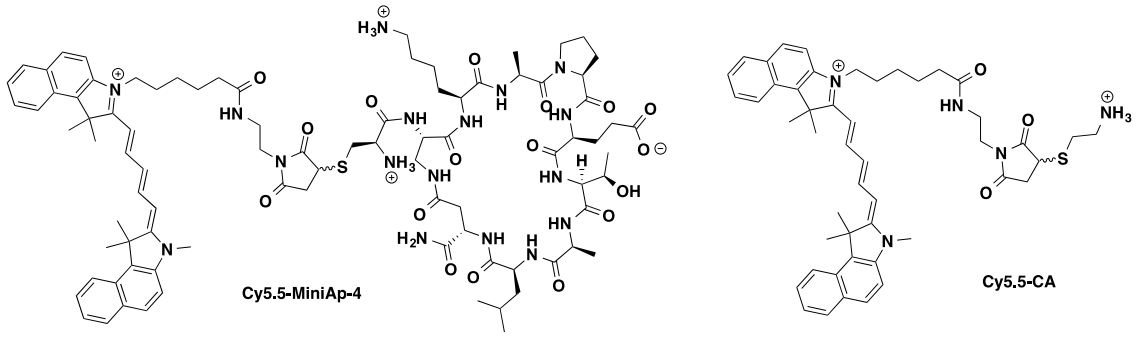

Figure S10. Molecular structures of injected compounds.

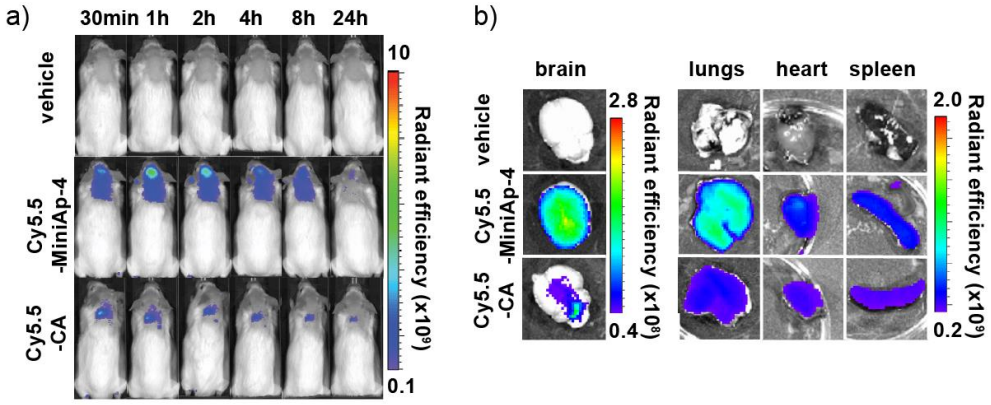

Figure S11. Fluorescence images taken in the IVS chamber of a) living anesthetized animals and b) excised organs. Although the signal in liver and kidneys of both compounds saturated the CCD camera, comparable amounts of Cy5.5-MiniAp-4 and Cy5.5-CA were found in the liver after homogenization and extraction (not shown).

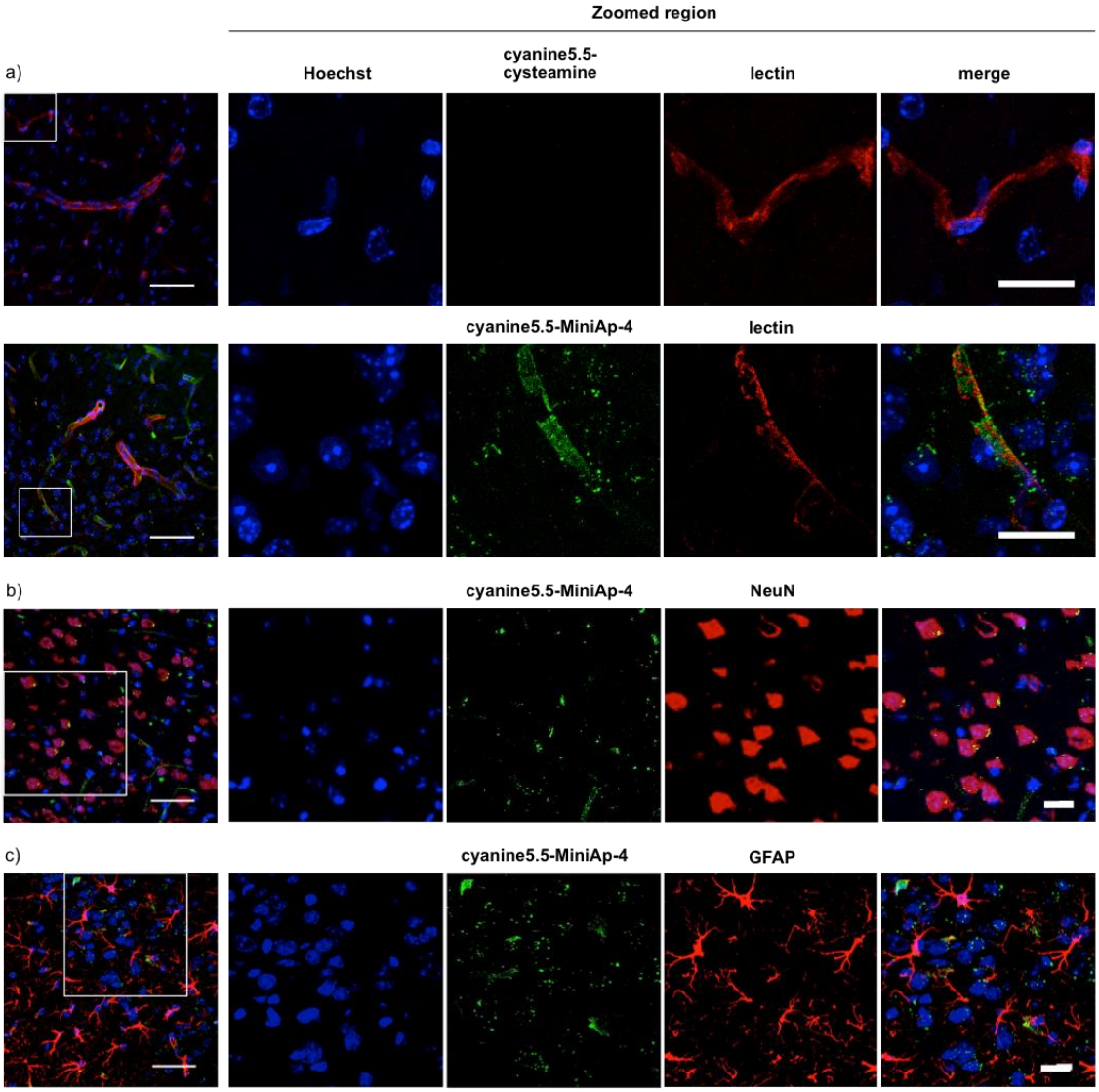

Figure S12. Representative confocal microscopy images of brain slices. Scale bar is 50 μm on the full images and 20 μm in the zoomed regions. In all images cell nuclei are shown in blue and Cy5.5 conjugates in green. a) Images from the same brain regions of mice injected with Cy5.5-CA (top) and Cy5.5-MiniAp-4 (bottom) are shown. Capillaries are displayed in red. b) Cy5.5-MiniAp-4 is observed in neurons. NeuN staining is shown in red. c) Cy5.5-MiniAp-4 is rarely seen in astrocytes. GFAP staining is shown in red.

Supplementary references

[1] E. Kaiser, R. L. Colescott, C. D. Bossinger, P. I. Cook, *Anal. Biochem.* **1970**, *34*, 595-598.

[2] T. Christensen, *Acta Chem. Scand.* **1979**, *33*, 763-766.

[3] S. Fiori, S. Pegoraro, S. Rudolph-Böhner, J. Cramer, L. Moroder, *Biopolymers* **2000**, *53*, 550-564.

[4] T.-L. Hwang, A. J. Shaka, *J. Magn. Reson., Ser. A* **1995**, *112*, 275-279.

[5] A. T. Brünger, P. D. Adams, G. M. Clore, W. L. DeLano, P. Gros, R. W. Grosse-Kunstleve, J. S. Jiang, J. Kuszewski, M. Nilges, N. S. Pannu, R. J. Read, L. M. Rice, T. Simonson, G. L. Warren, *Acta Crystallogr. D Biol. Crystallogr.* **1998**, *54*, 905-921.

[6] M. V. Berjanskii, S. Neal, D. S. Wishart, *Nucleic Acids Res.* **2006**, *34*, W63-69.

[7] R. A. Laskowski, M. W. MacArthur, D. S. Moss, J. M. Thornton, *J. Appl. Crystallogr.* **1993**, *26*, 283-291.

[8] R. Prades, S. Guerrero, E. Araya, C. Molina, E. Salas, E. Zurita, J. Selva, G. Egea, C. López-Iglesias, M. Teixidó, M. J. Kogan, E. Giralt, *Biomaterials* **2012**, *33*, 7194-7205.

[9] R. Cecchelli, S. Aday, E. Sevin, C. Almeida, M. Culot, L. Dehouck, C. Coisne, B. Engelhardt, M. P. Dehouck, L. Ferreira, *PLoS ONE* **2014**, *9*, e99733.

[10] J. Spengler, J. C. Jiménez, K. Burger, E. Giralt, F. Albericio, *J. Pept. Res.* **2005**, *65*, 550-555.

[11] C. Soto, E. M. Sigurdsson, L. Morelli, R. A. Kumar, E. M. Castaño, B. Frangione, *Nat. Med.* **1998**, *4*, 822-826.

[12] M. Schubert, D. Labudde, H. Oschkinat, P. Schmieder, *J. Biomol. NMR* **2002**, *24*, 149-154.

[13] D. Le-Nguyen, L. Chiche, F. Hoh, M. F. Martin-Eauclaire, C. Dumas, Y. Nishi, Y. Kobayashi, A. Aumelas, *Biopolymers* **2007**, *86*, 447-462.

[14] D. S. Wishart, C. G. Bigam, A. Holm, R. S. Hodges, B. D. Sykes, *J. Biomol. NMR* **1995**, *5*, 67-81.